



## Photoelectrochemical degradation of Methylene Blue with $\beta$ -PbO<sub>2</sub> electrodes driven by visible light irradiation

Guoting Li<sup>1,2</sup>, HoYin Yip<sup>2</sup>, Kin Hang Wong<sup>2</sup>, Chun Hu<sup>3</sup>, Jiuhui Qu<sup>3</sup>, Po Keung Wong<sup>2,\*</sup>

1. Department of Environmental and Municipal Engineering, North China University of Water Conservancy and Electric Power, Zhengzhou 450011, China. E-mail: [liguoting@ncwu.edu.cn](mailto:liguoting@ncwu.edu.cn)

2. School of Life Sciences, The Chinese University of Hong Kong, Shatin, N.T., Hong Kong SAR, China

3. State Key Laboratory of Environmental Aquatic Chemistry, Research Center for Eco-Environmental Sciences, Chinese Academy of Sciences, Beijing 100085, China

Received 23 June 2010; revised 01 December 2010; accepted 03 December 2010

### Abstract

$\beta$ -PbO<sub>2</sub> electrodes were prepared by electro-deposition and characterized by scanning electron microscopy, X-ray diffraction, X-ray photoelectron spectroscopy, and linear sweep voltammetry. We confirmed pure  $\beta$ -PbO<sub>2</sub> crystals were on the electrode and it had a high oxygen evolution potential. The photoactivity and photoelectrochemical (PEC) properties of the  $\beta$ -PbO<sub>2</sub> electrode were investigated under visible light irradiation ( $\lambda > 420$  nm) for the decolorization of Methylene Blue. Pseudo first-order kinetics parameter ( $K_{app}$ ) for dye decolorization using the  $\beta$ -PbO<sub>2</sub> electrode achieved  $6.71 \times 10^{-4} \text{ min}^{-1}$  under visible light irradiation, which indicated its excellent visible light-induced photoactivity. The  $K_{app}$  of the PEC process was as much as  $1.41 \times 10^{-3} \text{ min}^{-1}$  and was 1.71 times that of visible light irradiation or electrolysis even in the presence of the  $\beta$ -PbO<sub>2</sub> electrode. A significant synergetic effect was observed in the PEC system. We also employed TiO<sub>2</sub> modified  $\beta$ -PbO<sub>2</sub> electrodes in this test, which revealed that the TiO<sub>2</sub> immobilized on the  $\beta$ -PbO<sub>2</sub> electrode inhibited the visible light-induced PEC efficiency despite the amount of TiO<sub>2</sub> used for electrode preparation. The  $\beta$ -PbO<sub>2</sub> electrode was also superior to the dimensionally stable anode (Ti/Ru<sub>0.3</sub>Ti<sub>0.7</sub>O<sub>2</sub>) in visible light-induced photoactivity and PEC efficiency.

**Key words:** photocatalysis; photoelectrochemical process; visible light;  $\beta$ -PbO<sub>2</sub> electrode

**DOI:** 10.1016/S1001-0742(10)60489-5

**Citation:** Li G T, Yip HY, Wong K H, Hu Chun, Qu J H, Wong P K, 2011. Photoelectrochemical degradation of Methylene Blue with  $\beta$ -PbO<sub>2</sub> electrodes driven by visible light irradiation. Journal of Environmental Sciences, 23(6): 998–1003

### Introduction

Ultraviolet irradiation consists of only about 5% of total solar energy, while visible light accounts for as much as 45%. The need for utilizing solar light more efficiently becomes more and more urgent in terms of water splitting and decontamination of organic pollutants. While most studies on photocatalysts have focused on titania-based catalysts, TiO<sub>2</sub> only absorbs wavelengths near-UV regions ( $\lambda < 400$  nm). The common use of TiO<sub>2</sub> in photocatalysis is due to its non-toxic nature, high efficiency, and low cost. The commercialized P25 (TiO<sub>2</sub>) from Degussa has all the above-mentioned properties and is always employed as a reference/standard catalyst with the novel photocatalysts. In recent years, many novel non-titania photocatalysts such as In<sub>1-x</sub>Ni<sub>x</sub>TaO<sub>4</sub> ( $x$ : 0–0.2), CaBi<sub>2</sub>O<sub>4</sub>, PbBi<sub>2</sub>Nb<sub>2</sub>O<sub>9</sub> and NiO/SrBi<sub>2</sub>O<sub>4</sub> have been developed to utilize more solar energy in pathogenic bacteria disinfection, water splitting for H<sub>2</sub> production, and organic degradation or decontamination in water (Zou et al., 2001; Kim et al., 2004; Tang et al., 2004; Hu et al., 2006). The development

of effective and practical visible light-driven photocatalysts is regarded as the most important issue when dealing with difficulties related to photocatalysis.

However, both the titania-based and non-titania photocatalysts face the same problem of the rapid recombination of charge carriers – the photo-generated electrons (e<sup>-</sup>) and holes (h<sup>+</sup>), which leads to low quantum efficiency (Panov et al., 1998). In addition, the recovery and reuse of the photocatalyst has attracted much attention, with many studies immobilizing the photocatalysts on inert solid substrates to solve the recovery problem. Vinodgopal et al. (1993) reported that any process that could avoid the filtration step would be of great interest and other processes might also be helpful for photocatalytic oxidation (PCO). The attractive photoelectrochemical (PEC) process, which mainly consists of a photo-anode and an external electrical field, was developed with the aim to settle the two key problems. The photocatalyst can be immobilized on the photo-anode and the reclamation of the photocatalyst becomes unnecessary. Additionally, the external electric field across the photo-anode supplies an electrical bias on the photo-anode and enhances the

\* Corresponding author. E-mail: [pkwong@cuhk.edu.hk](mailto:pkwong@cuhk.edu.hk)

jesc.ac.cn

separation of photogenerated e<sup>-</sup> and h<sup>+</sup>. Consequently, the photoactivity of the immobilized catalyst is improved and the PEC process effectively degrades organic pollutants (Ward and Bard, 1982; Vinodgopal et al., 1993; Li et al., 2000; Pelegrini et al., 2001). Nevertheless, UV irradiation has always been involved in the PEC process, with only a few studies having focused on the visible light-induced PEC process (Solarska et al., 2005; Zhao and Zhu, 2006; Zhao et al., 2007; Li et al., 2007). The photoanodes employed are mainly made from established visible light-driven photocatalysts such as Bi<sub>2</sub>WO<sub>6</sub>, ZnWO<sub>4</sub> and  $\gamma$ -Bi<sub>2</sub>MoO<sub>6</sub>. Their PEC performance in relation to their stability and other properties requires further study as that of a dimensionally stable anode (DSA, Ti/Ru<sub>0.3</sub>Ti<sub>0.7</sub>O<sub>2</sub>) and PbO<sub>2</sub> anode. Dimensionally stable anodes are well accepted as a kind of electrode used in the chlor-alkali industry, which have also brought significant improvements in water electrolysis, selective synthesis, and destructive oxidation (Panizza et al., 2003). The PbO<sub>2</sub> anode is also effective for oxidizing pollutants and has been subjected to wide investigations (Chen, 2004), which have reported a bandgap of 1.7 eV and an equivalent wavelength of 729 nm (Stumm, 1992). This suggests that PbO<sub>2</sub> might be a prominent visible light induced photocatalyst. Meanwhile, PbO<sub>2</sub> electrodes, especially  $\beta$ -PbO<sub>2</sub> electrodes, are an excellent electrocatalysis material used in electrosynthesis and wastewater treatment. Studies show that PbO<sub>2</sub> has electrical conductivity similar to that of metals and it is characterized as a high oxygen evolution potential and low cost (Chen, 2004). Compared with PbO<sub>2</sub>, photo-anode material such as Bi<sub>2</sub>WO<sub>6</sub> may be not as stable and highly efficient as that of the popular electrocatalysis electrode in the PEC process. In this study,  $\beta$ -PbO<sub>2</sub> electrodes were prepared by electro-deposition and used in the PEC process for the degradation of Methylene Blue (MB) under visible light illumination. Both TiO<sub>2</sub> modified  $\beta$ -PbO<sub>2</sub> and DSA electrodes, which were reported to have performed efficiently with UV irradiation (Li et al., 2006), were also employed for comparison with pure  $\beta$ -PbO<sub>2</sub> electrode on their capabilities of photocatalytic and PEC oxidation. Methylene Blue is typically used in determining the photoactivity of novel photocatalysts under visible light irradiation, therefore, it was employed in this study.

## 1 Materials and methods

### 1.1 Materials

Methylene Blue (MB) (C<sub>16</sub>H<sub>18</sub>ClN<sub>3</sub>S) with a dye content of approximate 89% was purchased from Sigma (Fig. 1 for chemical structure), and used without further

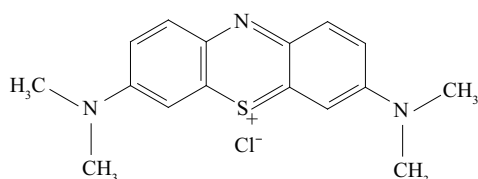


Fig. 1 Chemical structure of Methylene Blue (C.I. 52015).

purification. Other chemicals used were all of analytical grade. The commercial DSA electrode was provided by Beijing Titanium Industrial and Trade Company and was of similar size to that of the  $\beta$ -PbO<sub>2</sub> electrode.

### 1.2 Preparation and characterization of modified and unmodified $\beta$ -PbO<sub>2</sub> electrode

Preparation of the  $\beta$ -PbO<sub>2</sub> electrodes and TiO<sub>2</sub> modified  $\beta$ -PbO<sub>2</sub> electrodes was per our previous work (Li et al., 2006). Briefly, the 0.1 g TiO<sub>2</sub> and 2.0 g TiO<sub>2</sub> modified  $\beta$ -PbO<sub>2</sub> electrodes signify that the amount of TiO<sub>2</sub> used in 200 mL of electro-deposition solution were 0.1 g and 2.0 g when preparing the modified electrodes. The more TiO<sub>2</sub> used in electro-deposition solution, the more TiO<sub>2</sub> was immobilized on the modified electrodes examined in the test. Linear sweep voltammetric (LSV) experiments were conducted in a three electrode cell containing a Pt counter electrode and a saturated calomel electrode (SCE) was used as a reference on a basic electrochemical system (263 potentiostat, M270 electrochemical analysis software, EG&G, USA). Morphology of the electrode was characterized by a scanning electron microscope (KYKY2800, Chinese Academy of Sciences) with an acceleration voltage of 20 kV. The X-ray diffraction (XRD) patterns were recorded on a D8 Advance X-diffractometer (Cu K $\alpha$ ,  $\lambda$  = 0.15406 nm) (Bruker, Germany). The X-ray photoelectron spectroscopy (XPS) data were collected on an ESCA-Lab-220i-XL spectrometer with monochromatic Al K $\alpha$  radiation (1486.6 eV) (Thermo Scientific, Germany). The C1s peaks were used as an inner standard calibration peak at 284.7 eV.

### 1.3 Degradation of Methylene Blue by different processes

The photoactivity of the  $\beta$ -PbO<sub>2</sub> electrode was measured by degrading MB in aqueous solution. The reaction time was maintained for 60 min. A 100-W tungsten halogen lamp was used as the light source and a glass filter was passed through to cut off wavelengths shorter than 420 nm (light intensity 50 mW/cm<sup>2</sup>). The distance between the lamp and the reactor was 85 mm. These reactions were carried out in a semi-cylindrical quartz reactor. The available volume of the reactor was 150 mL and 125 mL of MB (7 mg/L) solution was added. The concentration of the dye was determined by measuring the absorbance at a fixed wavelength (665 nm), which corresponded to the maximum absorption wavelength. The stable voltage was supplied by a DH1715A-3 potentiostat (Beijing Dahua Radio Instrument Factory, China).

## 2 Results and discussion

### 2.1 Surface morphology and crystalline structure of $\beta$ -PbO<sub>2</sub> electrode

PbO<sub>2</sub> electrode is one of the most widely investigated anode materials for electrochemical oxidation due to its chemical stability, high electronic conductivity, and low cost of material (Chen, 2004). It is easily prepared by

anodic polarization of lead metal or by electro-deposition on different substrates (Quiroz et al., 2005). The  $\beta$ - $\text{PbO}_2$  electrode employed here had a tetragonal structure and  $\text{PbO}_2$  crystals on the electrode were compact and homogeneous (Fig. 2).  $\beta$ - $\text{PbO}_2$  has a high oxygen evolution overvoltage and it is always formed at very low pH conditions by electro-deposition (Ruetschi and Cahan, 1958). Therefore, a 0.1 mol/L  $\text{HNO}_3$  solution was employed for the preparation of the  $\beta$ - $\text{PbO}_2$  electrode in this study.

The crystalline structure was confirmed to be bulk  $\beta$ - $\text{PbO}_2$  crystals and no other impurity peaks judged from the existence of the main diffraction peaks at  $2\theta$  of  $25.4^\circ$ ,  $32.0^\circ$ ,  $36.2^\circ$ ,  $49.0^\circ$  and  $62.45^\circ$  (Fig. 3).  $\beta$ - $\text{PbO}_2$  electrode was more efficient than  $\alpha$ - $\text{PbO}_2$  for phenol degradation (Abaci et al., 2005), and therefore would be more favorable for the PEC process. The X-ray diffraction pattern of 2.0 g  $\text{TiO}_2$  modified  $\beta$ - $\text{PbO}_2$  electrode reported in previous research also suggested the prevailing existence of  $\beta$ - $\text{PbO}_2$  electrodes instead of other oxide species (Li et al., 2006).

## 2.2 X-ray photoelectron spectroscopy spectra of $\beta$ - $\text{PbO}_2$

X-ray photoelectron spectroscopy (XPS) was performed to acquire detailed information on the chemical states of

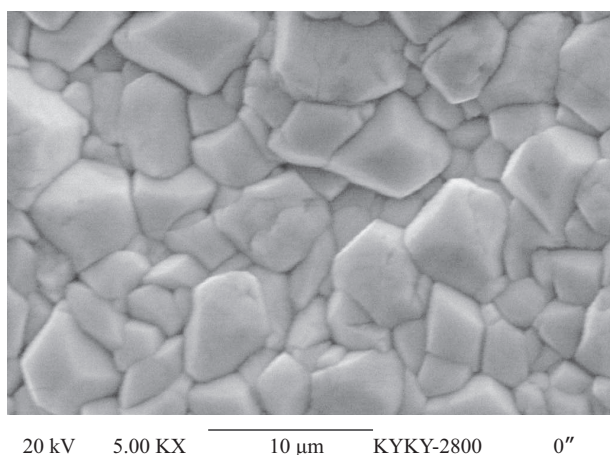


**Fig. 2** Scanning electron microscopy (SEM) image of  $\beta$ - $\text{PbO}_2$  electrode prepared by electro-deposition.

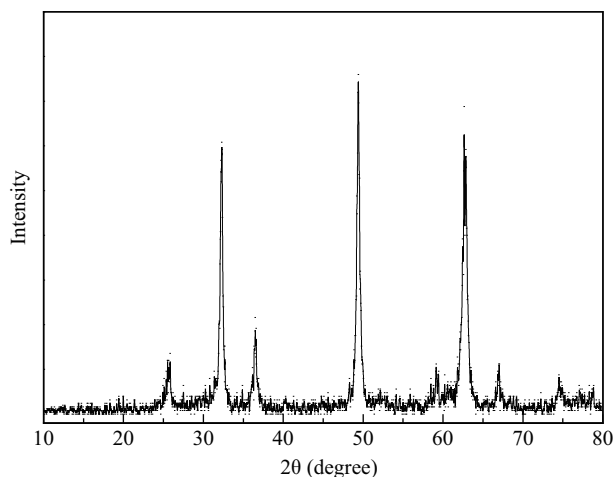


**Fig. 3** X-ray diffraction (XRD) pattern of  $\beta$ - $\text{PbO}_2$  electrode prepared by electro-deposition.

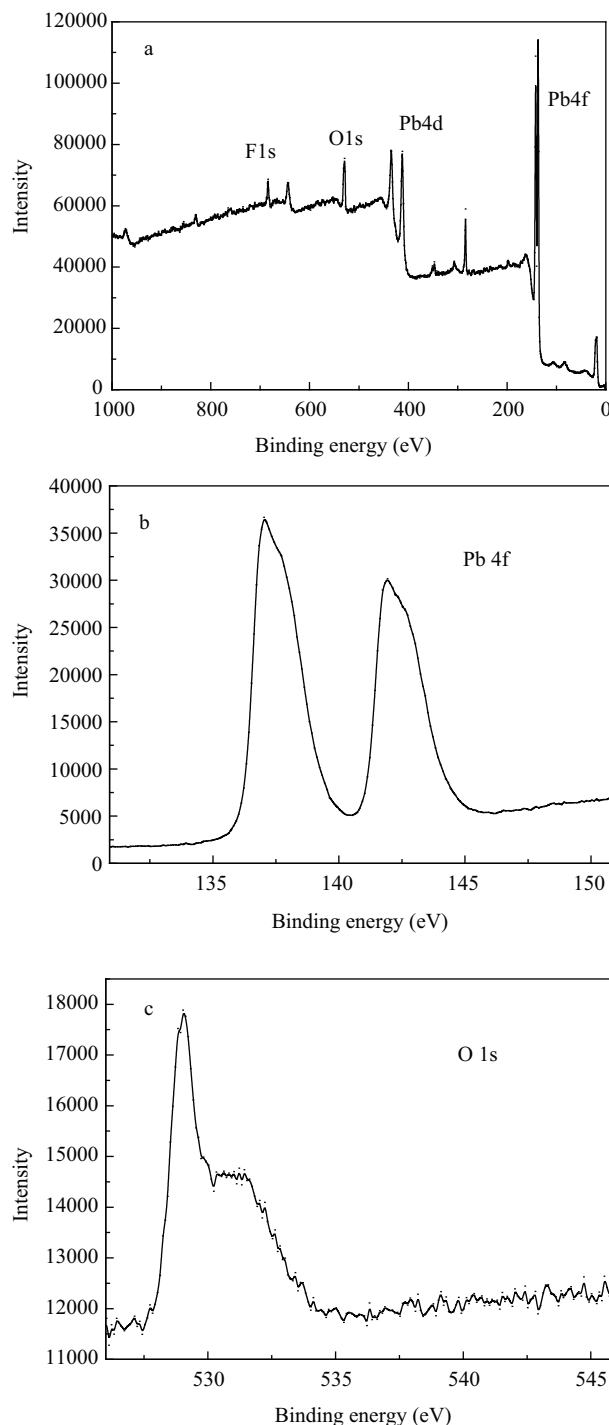


**Fig. 4** X-ray photoelectron spectroscopy (XPS) analysis of  $\beta$ - $\text{PbO}_2$  electrode. (a) general scan of  $\beta$ - $\text{PbO}_2$  electrode; (b) Pb 4f spectrum; (c) O 1s spectrum.

the cations and anions. Figure 4a shows the general survey spectrum of the  $\beta$ - $\text{PbO}_2$  layer and reveals that the surface layer contained Pb, O, and F elements. This is consistent with the composition of the electro-deposition employed for electrode preparation. Figure 4b, c shows the XPS spectra of Pb 4d, Pb 4f and O 1s regions. The Pb 4f spectra for the lead oxide layer exhibited two peaks centered at 137.0 and 141.9 eV. Its binding energy difference was equal to the difference reported by Morales et al. (2006) of 137.7 and 142.6 eV corresponding to  $4f_{7/2}$  and  $4f_{5/2}$ , respectively, which was consistent with the spectral values

for PbO<sub>2</sub>. The characteristic spectral peak attributed to the Pb 4f of PbO at around 139.0 eV was not found in the general scan. The Pb 4f<sub>7/2</sub> satellite peaks characterizing Pb<sup>2+</sup>, which are usually centered at about 138.1–138.6 eV, were not observed, which suggests there were no PbO and Pb<sub>3</sub>O<sub>4</sub> impurities on the electrode layer (Gupta et al., 1996; Wu et al., 2006). The collected spectra of O1s region showed two peaks. The peak at the lower binding energy of 529.1 eV was assigned to the lattice oxygen atoms directly bound to Pb of PbO<sub>2</sub>, while the broader peak at higher binding energy was attributed to the interaction of water oxygen with oxygen vacancies at the oxide surface (Amadelli et al., 1999).

### 2.3 Linear sweep voltammetry of $\beta$ -PbO<sub>2</sub> electrode

Cyclic voltammetry scans of Pt and the  $\beta$ -PbO<sub>2</sub> electrode in 0.1 mol/L Na<sub>2</sub>SO<sub>4</sub> electrolyte solution at pH 7.0 were performed in a three electrode system, with a platinum plate as a counter electrode and a standard calomel electrode as a reference electrode, respectively. The linear sweep voltammetry curves are illustrated in Fig. 5. The anodic current increased sharply with positive voltage and the onset potential for oxygen evolution for Pt and  $\beta$ -PbO<sub>2</sub> electrode was as high as 1.5 and 1.8 V, respectively. This indicated that the  $\beta$ -PbO<sub>2</sub> electrode with a high oxygen evolution potential was superior to the Pt electrode and should have good activity for pollutant oxidation.

### 2.4 Photoactivity of $\beta$ -PbO<sub>2</sub> electrode assisted by electrical field under visible light

The effect of visible light irradiation (> 420 nm) and electrical field was investigated and the pseudo first-order kinetics parameters ( $K_{app}$ ) of decolorization processes are presented in Table 1. Firstly, visible light irradiation alone had no decolorization effect on MB, but UV irradiation has been effective on the decolorization of Acid Orange 7 (Li et al., 2006). This indicates that visible light was too weak to decolorize dye directly. Once the  $\beta$ -PbO<sub>2</sub> electrode was applied with visible light in the same reactive system, however, the reaction rate coefficient achieved as much as

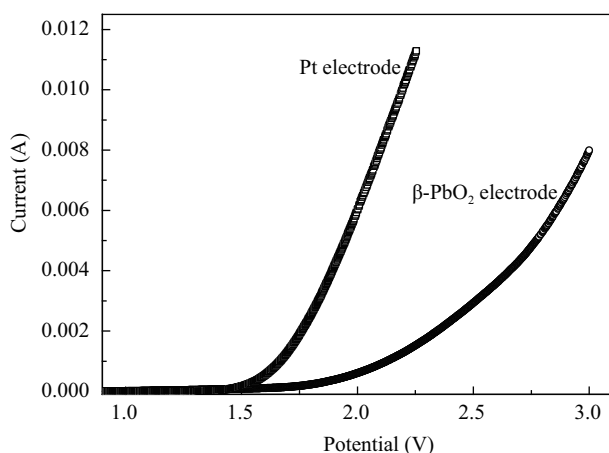


**Fig. 5** Anodic linear sweep voltammetry of Pt electrode and  $\beta$ -PbO<sub>2</sub> electrode in 0.1 mol/L Na<sub>2</sub>SO<sub>4</sub> electrolyte solution at pH 7.0 with a buffer of Na<sub>2</sub>HPO<sub>4</sub>/NaH<sub>2</sub>PO<sub>4</sub>, scan rate 50 mV/esc.

**Table 1** Kinetics parameters for different degradation methods<sup>a</sup>

Degradation method	$K_{app}$ ( $\times 10^{-3} \text{ min}^{-1}$ )	$R^2$
Photoelectrochemical process	1.41	0.99
Electrolysis	0.152	0.99
Visible light irradiation	0	0.99
Electrode with visible light	0.671	0.99

<sup>a</sup> 1.5 V potential was applied across the electrodes when needed, at neutral pH condition.

$6.71 \times 10^{-4} \text{ min}^{-1}$ , which showed that the  $\beta$ -PbO<sub>2</sub> crystals were photoactive to visible light. Furthermore, the reaction rate coefficient increased to  $1.41 \times 10^{-3} \text{ min}^{-1}$  after applying an electrical field of 1.5 V across the electrodes in the same reactive system of  $\beta$ -PbO<sub>2</sub> electrode and visible light. The  $K_{app}$  of electrolysis alone was only  $1.52 \times 10^{-4} \text{ min}^{-1}$  and the total effect of visible light irradiation and electrical field (PEC) was 1.71 times that of visible light irradiation or electrolysis alone with the presence of an electrode. Therefore, a significant synergetic effect was observed in the reactive system as we found previously for 2.0 g TiO<sub>2</sub> modified  $\beta$ -PbO<sub>2</sub> electrodes assisted by electrical field and UV (254 nm) (Li et al., 2006). This has also demonstrated that  $\beta$ -PbO<sub>2</sub> was capable of generating oxidizing agents when irradiated by visible light due to its small bandgap. We also investigated the recycle stability of  $\beta$ -PbO<sub>2</sub> electrodes by repeating MB photoelectrocatalytic degradation under the same experimental conditions. We observed that the reaction rate coefficient declined to  $6.53 \times 10^{-4} \text{ min}^{-1}$  on the fourth use for PEC degradation. This suggested that photoactivity decrease of  $\beta$ -PbO<sub>2</sub> electrode was not negligible.

The photoactivity of photo-anodes is a determining factor in the PEC process. The  $\beta$ -PbO<sub>2</sub> electrode was modified by TiO<sub>2</sub> to enhance its photoactivity and stability in our previous work, and here a series of TiO<sub>2</sub> modified  $\beta$ -PbO<sub>2</sub> electrodes and commercial DSA electrodes were compared in terms of their photoactivity driven by visible light (> 420 nm) and assisted by 1.5 V potential across the electrodes. The photoactivity of TiO<sub>2</sub> modified  $\beta$ -PbO<sub>2</sub> electrodes improved with increasing TiO<sub>2</sub> on the electrode under ultraviolet 254 nm irradiation and with 1.5 V potential across the electrodes. The photoactivity of the same series of modified  $\beta$ -PbO<sub>2</sub> electrodes was also investigated in the presence of visible light (> 420 nm) and 1.5 V potential across the electrodes, and PEC efficiencies decreased with increasing TiO<sub>2</sub> on the electrode (Fig. 6). It is widely accepted that TiO<sub>2</sub> is especially photoactive when the wavelength for irradiation is in the range of UV. As visible light (> 420 nm) employed was too weak to activate TiO<sub>2</sub>, there was almost no oxidizing agents generated for MB decolorization. The  $K_{app}$  for 0.1 g TiO<sub>2</sub> modified  $\beta$ -PbO<sub>2</sub> electrode was almost three times that of 2.0 g TiO<sub>2</sub> modified  $\beta$ -PbO<sub>2</sub> electrode and the  $K_{app}$  of the  $\beta$ -PbO<sub>2</sub> electrode was almost three times that of 0.1 g TiO<sub>2</sub> modified  $\beta$ -PbO<sub>2</sub> electrode under the experimental conditions examined above. These results indicate that the more PbO<sub>2</sub> on the electrode, the higher the decolorization rate achieved. It can be concluded that PbO<sub>2</sub> was the key parameter responsible for visible light for photocatalytic

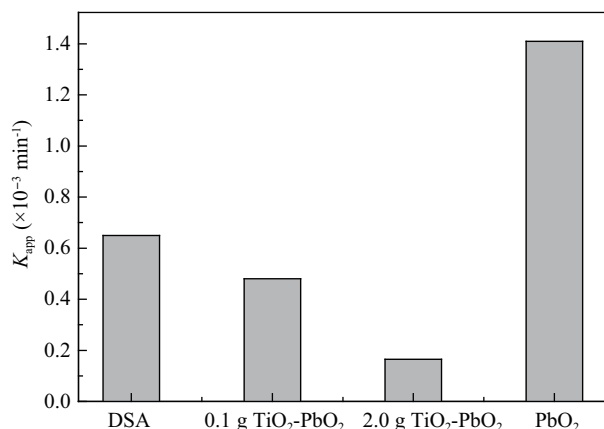


**Fig. 6** Pseudo first-order kinetics parameters ( $K_{app}$ ) for dimensionally stable anode (DSA, Ti/Ru<sub>0.3</sub>Ti<sub>0.7</sub>O<sub>2</sub>),  $\beta$ -PbO<sub>2</sub> electrode, 0.1 g TiO<sub>2</sub> and 2.0 g TiO<sub>2</sub> modified  $\beta$ -PbO<sub>2</sub> electrodes with visible light irradiation (> 420 nm), potential across the electrodes 1.5 V.

decomposing of MB. In addition, the  $K_{app}$  for commercial DSA electrodes under the experimental conditions were also higher than 0.1 g TiO<sub>2</sub> modified  $\beta$ -PbO<sub>2</sub> electrode but much lower than the pure  $\beta$ -PbO<sub>2</sub> electrode. The DSA electrode consists of 70% TiO<sub>2</sub> and 30% RuO<sub>2</sub>, with the high TiO<sub>2</sub> content limiting its photoactivity. Almost no photoactivity was observed for DSA and TiO<sub>2</sub> modified  $\beta$ -PbO<sub>2</sub> electrodes under visible light irradiation, while the  $K_{app}$  for the pure  $\beta$ -PbO<sub>2</sub> electrode amounted to  $6.71 \times 10^{-4} \text{ min}^{-1}$  indicating its excellent photoactivity by visible light. Thus, the  $\beta$ -PbO<sub>2</sub> electrode was a prominent photoanode under visible light illumination though it is well known as an excellent electrocatalysis electrode.

### 3 Conclusions

The  $\beta$ -PbO<sub>2</sub> electrode prepared by electro-deposition in this study was pure  $\beta$ -PbO<sub>2</sub> with a high oxygen evolution potential. The resulting  $\beta$ -PbO<sub>2</sub> electrode not only presented excellent photoactivity under visible light irradiation but also a significant synergetic effect in photoelectrochemical processes driven by visible light. The  $\beta$ -PbO<sub>2</sub> electrode was superior to the commercial DSA electrode in photocatalytic degradation of Methylene Blue as well as in the PEC process. By contrast, the photoelectrochemical activities of TiO<sub>2</sub> modified  $\beta$ -PbO<sub>2</sub> electrodes under the same experimental conditions were insignificant.

### Acknowledgments

This work was supported by a GRF grant (No. CUHK477610) of the Research Grants Council of Hong Kong SAR Government and the National Natural Science Foundation of China (No. 50708037).

### References

Abaci S, Tamer U, Pekmez K, Yildiz A, 2005. Performance of different crystal structures of PbO<sub>2</sub> on electrochemical degradation of phenol in aqueous solution. *Applied Surface Science*, 2409(1-4): 112–119.

Amadelli R, Armelao L, Tondello E, Daolio S, Fabrizio M,

Pagura C et al., 1999. A SIMS and XPS study about ions influence on electrodeposited PbO<sub>2</sub> films. *Applied Surface Science*, 142(1-4): 200–203.

Chen G H, 2004. Electrochemical technologies in wastewater treatment. *Separation and Purification Technology*, 38(1): 11–41.

Gupta S M, Kulkarni A R, Vedpathak M, Kulkarni S K, 1996. Surface study of lead magnesium niobate ceramic: using X-ray photoelectron spectroscopy. *Materials Science and Engineering B*, 39(1): 34–40.

Hu C, Hu X X, Guo J, Qu J H, 2006. Efficient destruction of pathogenic bacteria with NiO/SrBi<sub>2</sub>O<sub>4</sub> under visible light irradiation. *Environmental Science & Technology*, 40(17): 5508–5513.

Kim H G, Hwang D W, Lee J S, 2004. An undoped, single-phase oxide photocatalyst working under visible light. *Journal of American Chemical Society*, 126: 8912–8913.

Li G T, Qu J H, Zhang X W, Ge J T, 2006. Electrochemically assisted photocatalytic degradation of Acid Orange 7 with  $\beta$ -PbO<sub>2</sub> electrodes modified by TiO<sub>2</sub>. *Water Research*, 40(2): 213–220.

Li J P, Zhang X, Ai Z H, Jia F L, Zhang L Z, Lin J, 2007. Efficient visible light degradation of Rhodamine B by a photoelectrochemical process based on a Bi<sub>2</sub>WO<sub>6</sub> nanoplate film Electrode. *Journal of Physical Chemistry*, 111(18): 6832–6836.

Li X Z, Liu H L, Yue P T, Sun Y P, 2000. Photoelectrocatalytic oxidation of Rose Bengal in aqueous solution using a Ti/TiO<sub>2</sub> mesh electrode. *Environmental Science & Technology*, 34(20): 4401–4406.

Morales J, Petkova G, Cruz M, Caballero A, 2006. Synthesis and characterization of lead dioxide active material for lead-acid batteries. *Journal of Power Sources*, 158(2): 831–836.

Panizza M, Ouattara L, Baranova E, Comninellis C, 2003. DSA-type anode based on conductive porous *p*-silicon substrate. *Electrochemistry Communications*, 5(4): 365–368.

Panov G I, Uriarte A K, Rodkin M A, Sobolev V I, 1998. Generation of active oxygen species on solid surfaces. Opportunity for novel oxidation technologies over zeolites. *Catalysis Today*, 41(4): 365–385.

Pelegri R T, Freire R S, Duran N, Bertazzoli R, 2001. Photoassisted electrochemical degradation of organic pollutants on a DSA type oxide electrode: process test for a phenol synthetic solution and its application for the E1 bleach kraft mill effluent. *Environmental Science & Technology*, 35(13): 2849–2853.

Quiroz M A, Reyna S, Martínez-Huitle C A, Ferro S, De Battisti A, 2005. Electrochemical oxidation of *p*-nitrophenol from aqueous solutions at Pb/PbO<sub>2</sub> anodes. *Applied Catalysis B: Environmental*, 59(3-4): 259–266.

Ruetschi P, Cahan B D, 1958. Electrochemical properties of PbO<sub>2</sub> and the anodic corrosion of lead and lead alloys. *Journal of Applied Electrochemistry*, 105(7): 369–377.

Solarska R, Santato C, Jorand-Sartoretti C, Ulmann M, Augustynski J, 2005. Photoelectrolytic oxidation of organic species at mesoporous tungsten trioxide film electrodes under visible light illumination. *Journal of Applied Electrochemistry*, 35(7-8): 715–721.

Stumm W, 1992. Chemistry of Solid-water Interface: Processes at the Mineral-water and Particle-water Interface in natural Systems. John Wiley & Sons, New York. 347.

Tang J W, Zou Z G, Ye J H, 2004. Efficient photocatalytic decomposition of organic contaminants over CaBi<sub>2</sub>O<sub>4</sub> under visible-light irradiation. *Angewandte Chemie International*

- Edition*, 43: 4463–4466.
- Vinodgopal K, Hotchandani S, Kamat P V, 1993. Electrochemically assisted photocatalysis. TiO<sub>2</sub> particulate film electrodes for photocatalytic degradation of 4-chlorophenol. *Journal of Physical Chemistry*, 97(35): 9040–9044.
- Ward M D, Bard A J, 1982. Photocurrent enhancement via trapping of photogenerated electrons of TiO<sub>2</sub> particles. *Journal of Physical Chemistry*, 86: 3599–3605.
- Wu C Z, Hu S Q, Lei L Y, Yin P, Li T W, Xie Y, 2006.  $\beta$ -PbO<sub>2</sub> hollow nanostructures from the complex precursor: A self-produced intermediate template route. *Microporous and Mesoporous Materials*, 89(1-3): 300–305.
- Zhao X, Qu J H, Liu H J, Hu C, 2007. Photoelectrocatalytic degradation of triazine-containing azo dyes at  $\gamma$ -Bi<sub>2</sub>MoO<sub>6</sub> film electrode under visible light irradiation ( $\lambda > 420$  nm). *Environmental Science & Technology*, 41(19): 6802–6807.
- Zhao X, Zhu Y F, 2006. Synergetic degradation of Rhodamine B at a porous ZnWO<sub>4</sub> film electrode by combined electro-oxidation and photocatalysis. *Environmental Science & Technology*, 40(10): 3367–372.
- Zou Z G, Ye J H, Sayama K, Arakawa H, 2001. Direct splitting of water under visible light irradiation with an oxide semiconductor photocatalyst. *Nature*, 414: 625–627.